Spatial Beam Cleaning in Multimode GRIN Fibers: Polarization Effects

Mario Ferraro ⓘ *, Member, IEEE*, Fabio Mangini ⓘ *, Member, IEEE*, Mario Zitelli ⓘ, Raphael Jauberteau ⓘ, Yifan Sun ⓘ, Pedro Parra-Rivas ⓘ *, Member, IEEE*, Katarzyna Krupa ⓘ, Alessandro Tonello ⓘ, Vincent Couderc ⓘ, and Stefan Wabnitz ⓘ *, Senior Member, IEEE*

Abstract—The beam self-cleaning effect in graded-index multimode optical fibers has several interesting potential applications, such as high-resolution nonlinear imaging and mode-locked fiber lasers. Most experimental and theoretical studies of beam self-cleaning have neglected the role of the state of polarization of light. In this work, we fill this gap by reporting extensive experimental investigations of beam self-cleaning in multimode fibers, for beams with different input states of light polarization. We found that the state of polarization undergoes a complex evolution, which may lead either to full conservation of the input state of polarization, or to nearly complete light depolarization at the fiber output. The former outcome is compelling for applications based on the beam self-cleaning effect, such as multimode mode-locked fiber lasers for micromachining, and multimode devices for microscopy and endoscopy. The latter result, instead, permits to test the limits of validity of current purely scalar theoretical approaches for describing nonlinear propagation in multimode fibers.

Index Terms—Kerr effect, multimode fibers, nonlinear optics, polarization of light, self-cleaning.

I. INTRODUCTION

BEAM self-cleaning (BSC) is a surprising manifestation of the Kerr effect, leading to a power-induced

Mario Ferraro is with the Department of Information Engineering, Electronics and Telecommunications (DIET), Sapienza University of Rome, 00184 Rome, Italy, and also with Physics Department, University of Calabria, 87036 Rende, Italy.

Fabio Mangini, Mario Zitelli, Raphael Jauberteau, Yifan Sun, and Pedro Parra-Rivas are with the Department of Information Engineering, Electronics and Telecommunications (DIET), Sapienza University of Rome, 00184 Rome, Italy.

Katarzyna Krupa is with the Institute of Physical Chemistry, Polish Academy of Sciences, 01-224 Warsaw, Poland.

Alessandro Tonello and Vincent Couderc are with XLIM Institute (UMR CNRS 7252), University of Limoges, 87060 Limoges, France.

Stefan Wabnitz is with the Department of Information Engineering, Electronics and Telecommunications (DIET), Sapienza University of Rome, 00184 Rome, Italy, and also with CNR-INO, Istituto Nazionale di Ottica, 80078 Pozzuoli, Italy.

self-organization of the transverse intensity pattern emerging from graded-index (GRIN) multimode fibers (MMF). As a result of BSC, for input powers larger than a certain threshold value, one observes a transition from speckles into a Gaussian-like bell-shape [1], [2]. By exploiting BSC, MMF may deliver high-energy pulses while simultaneously maintaining the high beam quality of singlemode fibers. This is relevant for different applications, e.g., high power mode-locked MMF lasers [3], [4] and nonlinear imaging for microscopy and endoscopy [5], [6], [7].

Different physical mechanisms have been proposed for describing BSC in GRIN fibers, ranging from nonlinear nonreciprocity of mode coupling, self-organized criticality, to weak wave turbulence and classical condensation. An interesting approach based on the statistical mechanics of a photon gas permits a simplified description, based on a few thermodynamic parameters that obey an equation of state. Within this approach, BSC represents a state of thermal equilibrium, that is obtained from spatial four-wave-mixing-induced energy exchanges between modes, which play the role of particle collisions [8], [9], [10], [11]. The thermodynamic description is grounded on the existence of basic conservation laws, involving the optical power and momentum (both linear and angular) of the beam. Then BSC results from a steady-state distribution of the mode power population, which can be obtained from a principle of maximum entropy. Note that the definition of entropy is associated with the mode occupancy, and differs from that used in former works involving partially polarized waves [12]. This leads to the definition of two thermodynamic parameters, e.g., the temperature and the chemical potential, which unequivocally determine the state of equilibrium. Specifically, although the mode power fraction distribution associated with an MMF population might be highly complex for a speckled beam, whenever thermal equilibrium is reached, eventually this distribution approaches a steady-state law. Different experiments show that this asymptotic distribution can be well approximated by the Rayleigh-Jeans (RJ) law, i.e., the mode power fraction hyperbolically decays, as the mode propagation constant grows larger.

The thermodynamic approach to BSC is based on a scalar model for the statistics of a highly multimode fiber system. This is justified by the fact that, so far, experimental studies of BSC have been largely limited to the use of linearly polarized laser pulses at the fiber input. However, in general, the input state of polarization (SOP) is arbitrary; moreover, the SOP is
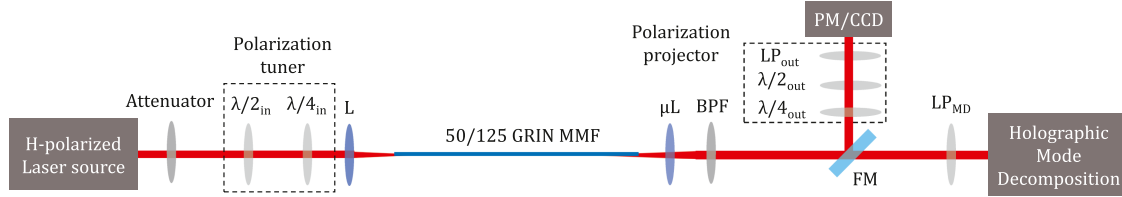
Fig. 1. Sketch of the experimental setup. The used MMF length varies between 2 and 20 m. The laser emits pulses of 1030 nm of wavelength. The pulse duration and the repetition rate can be varied between 174 fs and 2 ps, and between 100 kHz and 200 kHz, respectively. Acronyms stand for λ/2: half-waveplate; λ/4: quarter-waveplate; L: positive Lens; μL: positive microlens; BPF: bandpass filter (at the laser wavelength with a tolerance of 5 nm); LP: linear polarizer; FM: flipping mirror.

not conserved upon beam propagation in MMF. Indeed, the output SOP not only depends on the input SOP but, in general, on the injection conditions of light into the fiber, i.e., on the beam modal content [13]. Now, a purely scalar theory only holds in two limit cases, i.e., either when the SOP does not vary during the beam propagation, or if the propagating beam quickly depolarizes, regardless of the input SOP. In this regard, it has to be mentioned that Garnier et al. reported that light experiences repolarization at the occurrence of BSC [14]. In our experiments, we observed that both of these propagation regimes can be manifested. The former is achieved when exciting special input SOPs, which are found to act as principal modes of MMF. In this case, the degree of polarization (DOP) of light is preserved upon nonlinear beam propagation at the occurrence of BSC. On the other hand, in most cases a nearly complete depolarization of light occurs at the output of a few meters long GRIN fiber: this depolarization is enhanced by fiber nonlinearity. These observations are in agreement with previous experiments by Krupa et al., which demonstrated a reduction of the total DOP, along with a simultaneous increase of the degree of linear polarization (the input SOP being purely linear) [15].

In summary, in this work we present the results of a comprehensive experimental investigation of the dependence of BSC on the input SOPs of light, using different input pulse durations, ranging from a few picoseconds to hundreds of femtoseconds. Generally speaking, the SOP undergoes a complex evolution upon nonlinear beam propagation, which strongly depends on the light injection conditions into the fiber core. At high powers, the output DOP nearly vanishes at the fiber output, in analogy with the case of singlemode fibers [16], [17]. In this situation, a bell-shaped beam emerges in all polarization directions, with nearly the same mode content. However, we observed that if a laser beam is injected with a peculiar SOP, then nonlinear effects lead to a full re-polarization of the output light at the occurrence of BSC. In this sense we provide a validation of scalar models for BSC. For instance, within the thermodynamic framework, one can associate a self-cleaned beam with a unique value of temperature and chemical potential. Furthermore, our results permit to conciliate former experiments by Garnier et al. and Krupa et al., which reported that BSC can be accompanied by the observation of either an increase or a reduction of the DOP of light at the output of a GRIN fiber, as the input power grows larger [14], [15].

II. EXPERIMENTAL DETAILS

Our experimental setup is schematically shown in Fig. 1. Light pulses emitted with a repetition rate of either 100 or 200 kHz and a center wavelength of 1030 nm by a Yb-based laser (Light Conversion PHAROS-SP-HP) were injected straight onto the axis of a standard 50/125 GRIN MMF from Thorlabs by means of a piano-convex lens (L). We carried out experiments with both 2 m and 20 m long fiber spans, and found the same qualitative behavior for the evolution of the SOP. Therefore, in the following, we only report the experimental results that were obtained with the 2 m long fiber. We used sech pulses with a time duration of either 174 fs or 2 ps. At the fiber input, the laser beam had a nearly Gaussian spatial profile, while the input SOP was adjusted by means of a half- and a quarter-waveplate (λ/2$_{in}$ and λ/4$_{in}$, respectively).

At the fiber output, the beam is collected by means of a microlens (μL), and is split along two optical paths using a flipping mirror (FM). Since we used intense short pulses that may provide significant nonlinear spectral broadening, we inserted a bandpass filter (BPF) right after the μL. In this way, we could filter out possible losses of temporal coherence, which might artefact the spatiotemporal characterization of the output beam. The FM reflects the beam towards either a power meter (PM, S122 C Standard Photodiode Power Sensor from Thorlabs) or a CCD camera (Gentec Beamage-4M-IR). Downstream of the FM we inserted a polarization analyzer, which is composed of a quarter-waveplate (λ/4$_{out}$), a half-waveplate (λ/2$_{out}$), and a linear polarizer (LP$_{out}$). By appropriately selecting the orientation of the optical axes of such optical components, it is possible to determine the Stokes parameters associated with the SOP of the output beam. Specifically, one can separate the intensity of the field component with either vertical, horizontal, 45° oriented, or circular polarization, which are dubbed as I_1, I_1', I_2, and I_3, respectively. In this way, the Stokes parameters are given by $S_1 = (I_1 - I_1')/(I_1 + I_1')$, $S_2 = (2I_2 - I_1 - I_1')/(I_1 + I_1')$, and $S_3 = (2I_3 - I_1 - I_1')/(I_1 + I_1')$, which are associated with the horizontal/vertical, 45°/−45°, and right-circular/left-circular polarization, respectively. Finally, the total DOP is given by $\nu = \sqrt{S_1^2 + S_2^2 + S_3^2}$. When the FM is flipped, i.e., light is not reflected, the beam is sent to a holographic mode decomposition (MD) setup. The working principle of the latter is fully described in an article by Gervaziev et al. [18]. Such a holographic MD tool only works with linearly polarized light.
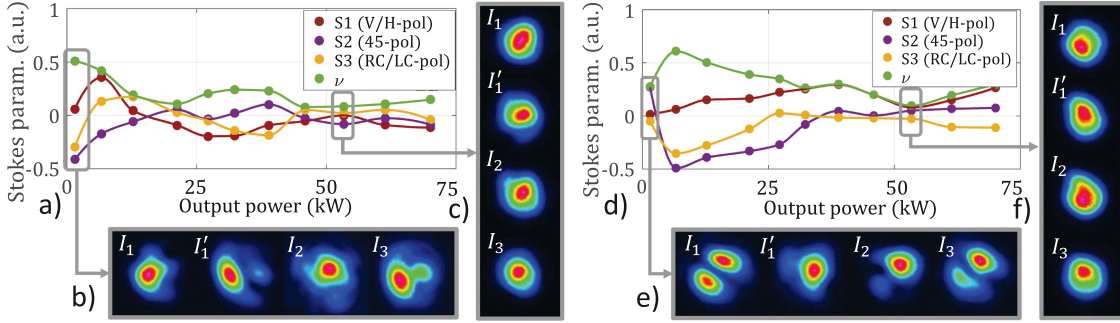
Fig. 2. Evolution of the SOP during BSC. (a)–(c) Vertical input polarization. (a) Evolution of the Stokes parameters vs. input peak power. (b) Near-field profile associated with different SOPs at the lowest input power. (c) Same as (b) at $P_p = 207.5$ kW. (d)–(f) Same as (a)–(c) with circular input polarization.

Therefore, we inserted a linear polarizer (LP$_{MD}$) right before the MD set-up. Note also that the BPF is necessary for the MD analysis, since our holographic MD tool requires to operate with nearly monochromatic light.

III. RESULTS

A. Evolution of DOP vs. Input Power

We carried out our first set of experiments by using 174 fs pulses injected into a 2 m long GRIN MMF, with a repetition rate of 100 kHz and either vertical or circular SOP. Let us consider the case of vertical input SOP first: in Fig. 2(a), we show the evolution, as a function of the input peak power (P_p), of the Stokes parameters of the laser beam at the fiber output. As it can be seen, one observes non-trivial changes of the SOP: all of the Stokes parameters S_1, S_2, and S_3 undergo large amplitude oscillations when P_p grows higher.

These SOP variations testify of a complex evolution associated with nonlinear beam propagation in the MMF: at low powers the output DOP is about 50%, owing to the effect of linear random-mode-coupling or weak disorder. In spite of being purely linear, these effects play a paramount role in determining the nonlinear dynamics of the beam [14], [19], [20]. Note that the curves reported in Fig. 2 are associated with relatively high input peak powers, i.e., of the order of a few hundred kilowatts, while the usual power threshold for BSC is of a few kilowatts. This can be seen in Fig. 2(b), where we show the output transverse spatial intensity patterns associated with the intensities I_1, I_1', I_2, and I_3 for $P_p = 6.8$ kW. Indeed, even at this relatively low input peak power we found that, when projected along the input polarization direction, the beam has already experienced BSC (pattern associated with I_1). Whereas, when projected in any other direction, the beam still exhibits some speckled features. A different behavior is instead found at higher input peak powers. In particular, within our experimental conditions, we found that the minimum DOP (green curve in Fig. 2(a)) is reached at $P_p \simeq$ 200 kW. Specifically, we found $\nu_{min} \simeq 8\%$. Correspondingly, the beam reaches a state of "full" cleaning, i.e., its associated intensity pattern has a bell-shape, regardless of the SOP projection at the fiber output (see Fig. 2(c)). Then, if the input power keeps growing, the beam undergoes re-polarization, and the cleaning effect is progressively lost (not shown here). This is

the fingerprint of the correlation between the SOP of a light beam and its mode content, thanks to which it is possible to obtain a full control of the output SOP by only varying the beam modal content at the fiber input in the linear propagation regime [13]. Here, we observed that, owing to the Kerr nonlinearity, the SOP at the fiber output evolves without changing the output mode power fraction.

Analogous results are found when using circularly polarized light at the fiber input. The corresponding results are shown in Fig. 2(d)–(f). Again, the DOP reaches its global minimum at around $P_p = 200$ kW. Moreover, for such an input power value, the beam has a bell-like shape along all polarization directions. Whereas at lower powers, the beam is still far from a bell shape in some polarization directions (see the difference between Fig. 2(e) and (f)).

It is interesting to note that, in the case of vertical input SOP (Fig. 2(a)–(c)), the Stokes parameter S_1 is negligible with respect to S_2 and S_3, although the I_1 spatial profile has a bell-like shape. Similarly, in Fig. 2(d)–(f), the Stokes parameter S_3 which corresponds to the input SOP, is negligible at the lowest input peak power value. However, in this case, the cleanest beam profile is obtained when projecting the beam along the horizontal axis (panel I_1' in Fig. 2(e)). Moreover, we found that, at variance with the case of input circular polarization, whenever the input light is vertically polarized, the maximum DOP at the fiber output is obtained for the lowest input peak power value. These differences between the cases of input linear or circular input SOP seem to indicate that only the fully depolarized self-cleaned beam provides a unique (that is, irrespective of the input SOP) steady-state solution for the complex evolution of the SOP at the fiber output. As we will see in the following, this aspect, which might appear secondary, is instead crucial for the validity of a thermodynamic approach for the description of the BSC effect.

B. Nonlinear Principal States of Polarization

Remarkably, in our experiments we have unveiled that special input SOPs exist, such that the beam remains highly polarized at the GRIN fiber output, even in the highest peak power regimes. These correspond to a virtual neutral axis of the MMF fiber, in analogy to that of single-mode fibers. At variance with the latter, however, the neutral axis depends on the input modal content,
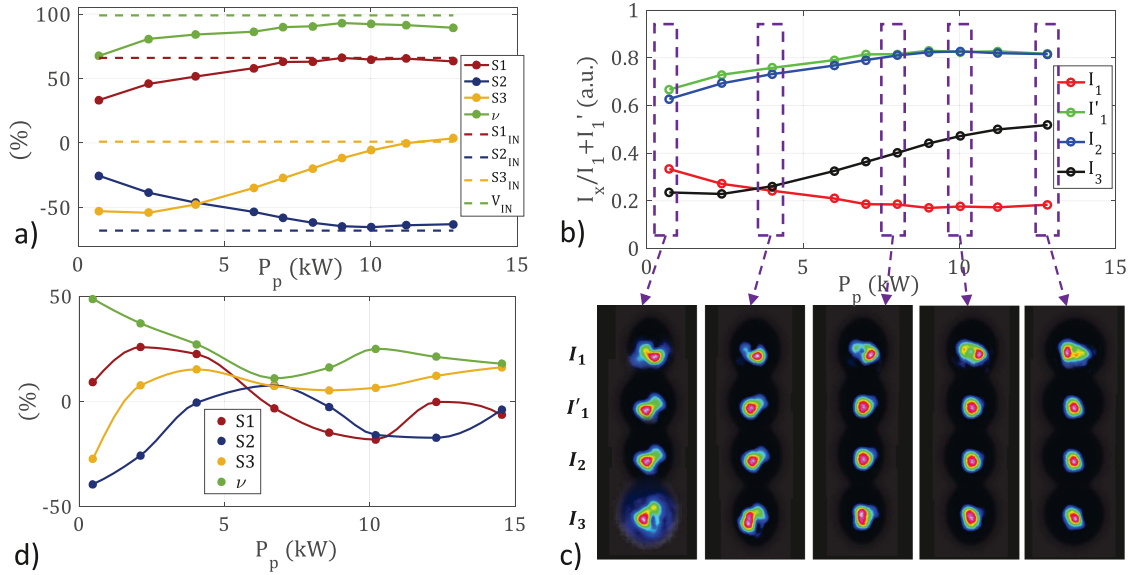
Fig. 3. (a) Stokes parameters and DOP vs input peak power. (b) Measured intensities, which are used to calculate the Stokes parameters in (a), normalized to the output power. (c) Near-fields for the five different input peak powers as highlighted in panel (b). (d) Same as (a) with different injection conditions providing the same injection efficiencies and same input SOP.

and it only exists above a certain power threshold, like the BSC effect.

The results are shown in Fig. 3, where we reported an experiment carried out with a 2 m long GRIN MMF with 50 (125) μm core (cladding) diameter, when injecting horizontally polarized laser pulses of 2 ps temporal duration at 200 kHz of repetition rate. As it can be seen in Fig. 3(a), we found an opposite trend of ν vs. P_p with respect to Fig. 2, i.e., the DOP increases as the input peak power grows larger, reaching a value quite close to 100% at $P_p = 12.5$ kW. Moreover, at such power value, the output SOP (dots connected by solid lines in Fig. 3(a)) approaches the input SOP (dashed lines in Fig. 3(a)). Hence, when experiencing BSC, a light beam which is injected with such a peculiar (elliptical) SOP, fully re-polarizes owing to the Kerr nonlinearity. As such, this unique SOP represents the self-cleaned *nonlinear eigenpolarizations* of the multimode GRIN fiber, i.e., the nonlinear principal state of polarization. We emphasize that the result in Fig. 3(a) shows the case of a linear eigenpolarization state, being $S_3 \simeq 0$ (cfr. dashed yellow line). However, in other experiments (not shown here) we observed that the eigen-SOP is generally elliptical.

The details of the evolution of the parameters I_1, I_1', I_2, and I_3 corresponding to Fig. 3(a) are shown in Fig. 3(b). Here, we normalized the values on the vertical axis to the output power, i.e., $I_1 + I_1'$. Whereas in Fig. 3(c), we show the beam profile associated with the parameters I_1, I_1', I_2, and I_3 at $P_p = 1, 4, 8$, 10, and 12.5 kW, respectively. In analogy with the condition of minimum DOP in Fig. 2, here we found that at the highest power, the beam acquires a bell-shape, which is nearly independent of the polarization projection at the fiber output.

Finally, it has to be mentioned that the nonlinear principal state of polarization strongly depends on fiber bending and on the injection conditions. As a matter of fact, we observed that if the fiber is squeezed without altering the input conditions, the

preservation of the input SOP at high powers is lost, and the beam experiences a depolarization, similar to Fig. 2. Moreover, when keeping the fiber untouched and without varying the input SOP, we found one and only one peculiar injection condition (we moved the fiber tip in the plane transverse to the laser direction), for which the nonlinear principal state of polarization was excited. For instance, in Fig. 3(d), we report the Stokes parameters as a function of the input peak power, within the same experimental conditions of Fig. 3(a), but with different injection conditions (we ensured anyway that the injection efficiency was nearly the same in the two cases). As it can be seen, the evolution of the SOP as a function of P_p is very different from what is reported in Fig. 3(a); instead of a full re-polarization, we observed a non-trivial evolution of ν, which reaches its minimum ($\nu_{min} \simeq 10\%$) at $P_p = 6$ kW, similarly to the experiments reported in Fig. 2.

C. Mode Decomposition: Validation of the Thermodynamic Approach to BSC

For comparing our experimental results with theoretical predictions, obtained from a thermodynamic approach for describing BSC, we performed a separate MD for each orthogonal polarization direction at the fiber output. The results, which are shown in Fig. 4, refer to a 2 m long GRIN MMF span, when injecting horizontally polarized laser pulses of 2 ps temporal duration. We emphasize that, at variance with picosecond pulses, when dealing with ultra-short pulses, like those in Fig. 2, strictly speaking the thermodynamic theory does not hold, since the peak power of the beam is not conserved, owing to dispersive pulse broadening. For instance, the peak power is reduced by about 4 times from the fiber input to the output within the experimental conditions in Fig. 2.
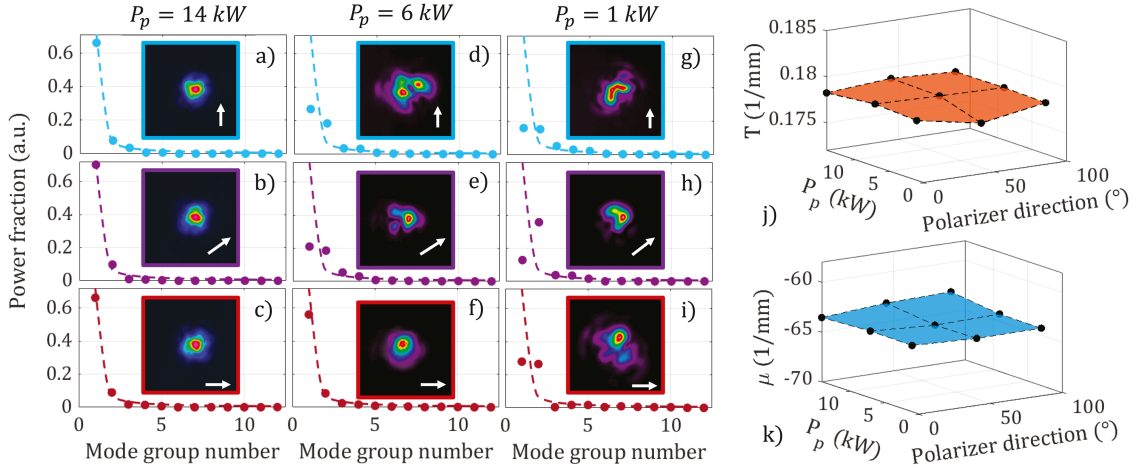
Fig. 4. Mode decomposition analysis during beam self-cleaning. (a)–(i) Mode power fraction as a function of the mode group number at different input peak powers, projected along different output polarization directions. Insets show the measured beam near-field at the fiber output. Arrows represent the orientation of the linear polarizer LP$_{MD}$. The dashed lines in (a)–(i) are a RJ law fit of the data in (a)–(c). (j)–(k) Temperature and chemical potential associated with the experimental mode power fraction distribution in (a)–(i).

In Fig. 4(a)–(i) we show the power fraction associated with each mode group, i.e., with the ensemble of modes having nearly the same propagation constant, for three different values of the input peak power, i.e., $P_p = 14$ kW (Fig. 4(a)–(c)), 6 kW (Fig. 4(d)–(f)), and 1 kW (Fig. 4(g)–(i)). Each row in Fig. 4(a)–(i) corresponds to a different SOP at the fiber output, i.e., to a different orientation of the LP$_{MD}$ in Fig. 1, as indicated by white arrows in the insets of Fig. 4(a)–(i). Specifically, data in Fig. 4(a), (d), and (g) refer to the vertical polarization, those in Fig. 4(b), (e), and (h) to 45° polarization, and those in Fig. 4(c), (h), and (i) to horizontal polarization, respectively. Finally, the insets of Fig. 4(a)–(i) show the near-field intensity profile at the fiber output, measured by means of a CCD camera.

When obtaining the results of Fig. 4, we paid particular attention to ensuring that the beam was injected without any appreciable tilt angle with respect to the fiber axis. This is a key condition for ensuring the occurrence of BSC on the fundamental mode [21], i.e., that the mode equilibrium distribution approaches a RJ law. The presence of a tilt angle, along with an offset with respect to the fiber axis would provide the beam with an orbital angular momentum, whose conservation leads to a modified mode equilibrium distribution [22], [23].

At $P_p = 14$ kW, BSC was observed for all output polarization directions. Besides the bell-shape presented in the inset, the reaching of a thermal equilibrium state is confirmed by the good fit of the mode power distribution with a RJ law (dashed curve in Fig. 4(a)–(c)). In order to allow for a clearer comparison among the data in Fig. 4(a)–(i), we report the RJ fit of Fig. 4(a)–(c) also in Fig. 4(d)–(i). At $P_p = 6$ kW, we found that a bell-shape was only obtained along the horizontal polarization, i.e., along the same polarization direction of light at the fiber input. Note that both results shown in Fig. 4(a)–(c) and 4(d)–(f) are in agreement with the experiment carried out with fs pulses, which is reported in Fig. 2(b) and (c). Finally, when the input peak power is too low, multimode interference produces a speckled pattern (Fig. 4(g)–(i)). In this case, the Kerr effect is not strong enough for reaching the BSC condition. Indeed, one can see

that only the dashed curve in Fig. 4(f) provides a good fit of the experimental data; whereas the mode power fractions are rather far from their equilibrium distribution in Fig. 4(d)–(i), i.e., they do not show a hyperbolic decay with the mode group number.

Finally, one may notice that the cyan, violet and red curves in Fig. 4 are rather similar. This is due to the fact that we found practically identical (within the experimental error) mode power distributions in Fig. 4(a)–(c), i.e., the beam can be considered fully depolarized at first approximation. As a result, the values of temperature (T) and chemical potential (μ) associated with the equilibrium RJ distribution are the same, regardless of the output polarization direction. Such a result is pivotal for providing a validation of the thermodynamic description of BSC. Such a confirmation, to the best of our knowledge, was not yet demonstrated. Indeed, since light power can flow between modes with different SOPs, one may only define a state of complete thermal equilibrium whenever light is fully depolarized at the fiber output.

We highlight that, as described by Wu et al. [24], the value of T and μ that the beam reaches at thermal equilibrium can be determined even in out-of-equilibrium states. Indeed, T and μ can be computed from the mode power fraction distribution. This theoretical expectation is experimentally verified in Fig. 4(j) and (k). There, we report the nine values of T and μ which are calculated from the mode power fraction distribution in Fig. 4(a)–(i). As it can be clearly appreciated, both T and μ are nearly constant, whatever the value of the input peak power or the orientation of the linear polarizer LP$_{MD}$.

IV. CONCLUSION

In conclusion, we carried out an extensive study of the nonlinear evolution of the SOP of picosecond and femtosecond laser pulses, which accompany the BSC effect in GRIN MMFs. Specifically, we demonstrated the possibility of achieving BSC when injecting elliptically polarized light at the fiber input.

Remarkably, we identified a previously un-noticed case of nonlinear full re-polarization of light, which can be ascribed to the presence of a nonlinear eigenpolarization of light in the highly multimode system. The understanding of this effect, which is akin to a *polarization condensation*, will require further theoretical studies. Fully polarized self-cleaned beams represent the nonlinear eigenpolarizations or principal states of the multimode fiber, which are excited with a specific laser injection condition, and may have interesting applications for stable multimode beam delivery and transmission.

To the contrary, for most of the laser injection conditions, the presence of BSC is associated with a significant nonlinear depolarization, which can be nearly complete at the highest powers that we tested (we reached a minimum DOP below 10%). In this regime, the output mode power distribution obeys the same RJ law, irrespective of the SOP. Interestingly, such a modal evolution is opposite to that reported in linear propagation regime by Xiong et al., who observed that the output SOP can be fully tuned via the input (and hence the output) modal content [13]. Our results validate the use of a scalar model for describing BSC as a manifestation of wave thermalization. Hence, MMFs provide an easily accessible test-bed for the experimental investigation of the entropy of nonlinear waves, e.g., for optical calorimetry experiments [25]. In terms of applications, our results are interesting for several MMF-based technologies, such as fiber lasers and multiphoton imaging devices.

REFERENCES

[1] K. Krupa et al., "Spatial beam self-cleaning in multimode fibres," *Nature Photon.*, vol. 11, no. 4, pp. 237–241, 2017.

[2] Z. Liu, L. G. Wright, D. N. Christodoulides, and F. W. Wise, "Kerr self-cleaning of femtosecond-pulsed beams in graded-index multimode fiber," *Opt. Lett.*, vol. 41, no. 16, pp. 3675–3678, 2016.

[3] U. Tegin, B. Rahmani, E. Kakkava, D. Psaltis, and C. Moser, "Single-mode output by controlling the spatiotemporal nonlinearities in mode-locked femtosecond multimode fiber lasers," *Adv. Photon.*, vol. 2, no. 5, 2020, Art. no. 056005.

[4] L. G. Wright, D. N. Christodoulides, and F. W. Wise, "Spatiotemporal mode-locking in multimode fiber lasers," *Science*, vol. 358, no. 6359, pp. 94–97, 2017.

[5] N. O. Moussa et al., "Spatiotemporal beam self-cleaning for high-resolution nonlinear fluorescence imaging with multimode fiber," *Sci. Rep.*, vol. 11, no. 1, pp. 1–8, 2021.

[6] S. Wehbi et al., "Continuous spatial self-cleaning in GRIN multimode fiber for self-referenced multiplex CARS imaging," *Opt. Exp.*, vol. 30, no. 10, pp. 16104–16114, 2022.

[7] T. Mansuryan et al., "Large band multiphoton microendoscope with single-core standard graded-index multimode fiber based on spatial beam self-cleaning," *Proc. SPIE*, vol. 12356, 2023, Art. no. 123560B, doi: 10.1117/12.2652346.

[8] M. Ferraro, F. Mangini, M. Zitelli, and S. Wabnitz, "On spatial beam self-cleaning from the perspective of optical wave thermalization in multimode graded-index fibers," *Adv. Phys.: X*, vol. 8, no. 1, 2023, Art. no. 2228018, doi: 10.1080/23746149.2023.2228018.

[9] F. Mangini et al., "Statistical mechanics of beam self-cleaning in GRIN multimode optical fibers," *Opt. Exp.*, vol. 30, no. 7, pp. 10850–10865, 2022.

[10] H. Pourbeyram et al., "Direct observations of thermalization to a Rayleigh-Jeans distribution in multimode optical fibres," *Nature Phys.*, vol. 18, pp. 685–690, 2022.

[11] K. Baudin et al., "Classical Rayleigh-Jeans condensation of light waves: Observation and thermodynamic characterization," *Phys. Rev. Lett.*, vol. 125, no. 24, 2020, Art. no. 244101.

[12] A. Picozzi, "Entropy and degree of polarization for nonlinear optical waves," *Opt. Lett.*, vol. 29, no. 14, pp. 1653–1655, 2004.

[13] W. Xiong, C. W. Hsu, Y. Bromberg, J. E. Antonio-Lopez, R. A. Correa, and H. Cao, "Complete polarization control in multimode fibers with polarization and mode coupling," *Light: Sci. Appl.*, vol. 7, no. 1, 2018, Art. no. 54.

[14] J. Garnier et al., "Wave condensation with weak disorder versus beam self-cleaning in multimode fibers," *Phys. Rev. A*, vol. 100, no. 5, 2019, Art. no. 053835.

[15] K. Krupa et al., "Nonlinear polarization dynamics of Kerr beam self-cleaning in a graded-index multimode optical fiber," *Opt. Lett.*, vol. 44, no. 1, pp. 171–174, 2019.

[16] B. Crosignani, B. Daino, and P. D. Porto, "Depolarization of light due to the optical Kerr effect in low-birefringence single-mode fibers," *J. Opt. Soc. Amer. B*, vol. 3, no. 8, pp. 1120–1123, Aug. 1986. [Online]. Available: https://opg.optica.org/josab/abstract.cfm?URI=josab-3-8-1120

[17] Q. Liu, L. Shi, P. Ho, and R. Alfano, "Nonlinear vector rotation and depolarization of femtosecond laser pulses propagating in non-birefringent single-mode optical fibers," *Opt. Commun.*, vol. 138, no. 1, pp. 45–48, 1997. [Online]. Available: https://www.sciencedirect.com/science/article/pii/S0030401897000448

[18] M. Gervaziev et al., "Mode decomposition of multimode optical fiber beams by phase-only spatial light modulator," *Laser Phys. Lett.*, vol. 18, no. 1, 2020, Art. no. 015101.

[19] G. Fu et al., "Beam self-cleaning of 1.5 μm high peak-power spatiotemporal mode-locked lasers enabled by nonlinear compression and disorder," *Laser Photon. Rev.*, vol. 17, no. 7, 2023, Art. no. 2200987.

[20] M. Zitelli et al., "Spatiotemporal mode decomposition of ultrashort pulses in linear and nonlinear graded-index multimode fibers," *Photon. Res.*, vol. 11, no. 5, pp. 750–756, 2023.

[21] E. Deliancourt et al., "Kerr beam self-cleaning on the LP_{11} mode in graded-index multimode fibers," *OSA Continuum*, vol. 2, no. 4, pp. 1089–1096, 2019.

[22] E. Podivilov et al., "Thermalization of orbital angular momentum beams in multimode optical fibers," *Phys. Rev. Lett.*, vol. 128, no. 24, 2022, Art. no. 243901.

[23] F. O. Wu, Q. Zhong, H. Ren, P. S. Jung, K. G. Makris, and D. N. Christodoulides, "Thermalization of light's orbital angular momentum in nonlinear multimode waveguide systems," *Phys. Rev. Lett.*, vol. 128, no. 12, 2022, Art. no. 123901.

[24] F. O. Wu, A. U. Hassan, and D. N. Christodoulides, "Thermodynamic theory of highly multimoded nonlinear optical systems," *Nature Photon.*, vol. 13, no. 11, pp. 776–782, 2019.

[25] M. Ferraro, F. Mangini, F. Wu, M. Zitelli, D. Christodoulides, and S. Wabnitz, "Calorimetry of photon gases in nonlinear multimode optical fibers," 2022, *arXiv:2212.12781*.